

# Experimental study of pressure drop and heat transfer in a U bend channel with various guide vanes and ribs

Susanna Ciminà<sup>2</sup>, Chenglong Wang<sup>1</sup>, Lei Wang<sup>1</sup>, Alfonso Niro<sup>2</sup>, Bengt Sunden<sup>1\*</sup>

<sup>1</sup>*Department of Sciences, Lund University, Box 118, Lund SE-22100, Sweden*

<sup>2</sup>*Department of Energy, Politecnico di Milano, Via Lambruschini 4, Milano IT - 20156, Italy*

*\*Corresponding author, Tel: +46-46-2228605; E-mail:*

[bengt.sunden@energy.lth.se](mailto:bengt.sunden@energy.lth.se)

## Abstract

An experimental study has been conducted to investigate the pressure drop and heat transfer in a U-bend section with various configurations of guide vanes and two kinds of shape of ribs on the outer wall. Ten different cases of guide vanes were tested. Results highlight that the use of special guide vanes can reduce the pressure drop penalty up to a maximum of 31%. However, the application of guide vanes is usually associated with the reduction of heat transfer. To further enhance the heat transfer, transverse and V-shaped ribs are attached on the outer wall. Thermal performance evaluation shows that the V - 45° downstream pointing ribs coupled with configuration 5 of the guide vanes give the best thermal performance. The results of this study can be employed to improve the internal design of the cooling system of modern gas turbine blades.

**Keywords:** Rough surfaces; structured roughness; single-phase flow; bend duct geometry; guide vanes; liquid crystal thermography

## Nomenclature

$c_p$	pressure drop coefficient
$D_h$	hydraulic diameter of the channel (m)
$e$	rib height (m)
$f$	Darcy friction factor, $f = \frac{(\Delta P/L)D_h}{\rho U_0^2/2}$
$f_0$	Darcy friction factor in a smooth straight channel, $f_0 = 0.316 \cdot Re^{-0.25}$
$h$	heat transfer coefficient ( $W m^{-2} K^{-1}$ )
$k$	thermal conductivity of air ( $W m^{-1} K^{-1}$ )
$L$	streamwise distance between pressure taps (m)
$Nu$	Nusselt number, $Nu = h \cdot D_h/k$
$\overline{Nu}$	area-averaged Nusselt number
$Nu_0$	Nusselt number in a smooth straight channel, $Nu_0 = 0.023 \cdot Re^{0.8} \cdot Pr^{0.4}$
$p$	rib pitch (m)
$\Delta P$	pressure drop (Pa)
$Pr$	Prandtl number of air
$q_w$	supplied heat flux ( $Wm^{-2}$ )
$q_{loss}$	heat loss ( $Wm^{-2}$ )
$Re$	Reynolds number, $Re = U_0 D_h/\nu$
$T_0$	air bulk temperature (K)
$T_w$	wall temperature (K)
$U_0$	air bulk velocity ( $ms^{-1}$ )
$W$	divider wall length (m)
$X$	streamwise direction

$Y$  spanwise direction  
 $Z$  wall-normal direction

### *Greek symbols*

$\eta$  thermal performance  
 $\mu$  dynamic viscosity ( $\text{kg m}^{-1}\text{s}^{-1}$ )  
 $\nu$  kinematic viscosity of air,  $\mu/\rho$ , ( $\text{m}^2\text{s}^{-1}$ )  
 $\rho$  density of air ( $\text{kg m}^{-3}$ )

## **Introduction**

In modern gas turbine engines improvement of the overall thermal efficiency and power output is continuously required. One way to achieve this goal is to increase the turbine inlet temperature (TIT) from the principles of engineering thermodynamics, Han et al. (2012). Currently gas turbine engines operate at high inlet temperature which far exceeds the allowable material temperature of turbine blades. Therefore, the blades must be cooled by extracting air from the last stage of the compressor through internal serpentine cooling passages, Sunden and Xie (2011). A key element is the serpentine cooling passages with 180-deg sharp turns, Han (2004). Due to the flow separation and strong secondary flow in the turn section, the flow structures and heat transfer are much more complex than those in a straight channel. Many studies have been conducted to investigate the heat transfer and fluid flow in the bend region. For example, Schabacker et al. (1998) carried out PIV measurements and showed a remarkable increase of the velocity in the turn region, with the consequence of jet impingement on the outer wall and the separated flow and recirculation region after the turn at the inner wall. Son et al. (2002) subsequently found that the flow impingement on the outer wall is the main factor for heat transfer enhancement, and the secondary flow which consists of two counter rotating vortices is closely connected to the improvement of the thermal performance. Other studies are exemplified by Metzger et al. (1984), Fan and Metzger (1987),

Metzger and Sahm (1986), and Metzger et al. (1988) in which the pressure loss and heat transfer in the rectangular passage sharp 180° turns were investigated. Ekkad and Han (1997) provided detailed heat transfer distributions in two-pass channels with rib turbulators.

The bend sections, due to the sharp turn, produce as high as 25% of the pressure loss in the entire serpentine cooling passages, Schüler et al. (2011). Therefore, it is imperative to reduce the pressure loss in the bend section. The integration of guide vanes in the turn section is expected to reduce the pressure loss while keeping the heat transfer levels high. However, the design and the position of these guide vanes in the flow path are essential for the successful application. Rao et al. (2004) as well as Rao and Prabhu (2004) studied the effect of the insert of single and multiple guide vanes (short and long in shape) in the 180° turn bend, in which 12 different configurations of single guide vanes and 10 different multiple guide vanes were tested. The results indicated that the shape and position of the guide vanes significantly affect the pressure loss. Specifically, long vanes located at the center of the bend decrease the overall pressure drop by as much as 40-45% compared to the no guide vane case within the bend. However, a reduction in overall pressure drop by only 15% was achievable through the use of guide vanes in rib-roughened square channels. Luo and Razinsky (2009) presented a numerical study of the turbulent flows in 2D and 3D U-bend geometries, with and without guide vanes. Their results showed that the vane placed in the midline of the U-duct can significantly reduce the pressure loss of about 50% due to the fact that the flow separation after the turn and the growth of secondary flow vortices were mitigated. Chen et al. (2011) studied the effect of turning vane configurations on the heat transfer and pressure drop in a ribbed internal cooling system. The results indicated that the heat transfer in the region after the turn was reduced by 35% compared to the baseline case without vanes. They also demonstrated that the installation of the ribs in the turn region with the presence of special guide vanes could enhance the heat transfer of about 15%.

To further reduce the pressure drop in the turn section, other interesting studies have been conducted. Schüler et al. (2011) showed that the pressure loss could be significantly reduced by about 25% in a ribbed rectangular two-pass channel by using an inner turning vane or a combination of inner and outer turning vanes. The reason is that the turning vane is helpful in preventing the formation of a recirculation zone on the inner wall after the turn. Another special way to reduce the pressure loss is to optimize the U-bend design. Coletti et al. (2013) presented a detailed numerical study to optimize the U-bend design and found that the increase of the bending radius can limit the acceleration in the first part of the turn and consequently reduce the recirculation area along the second half of the inner wall. Saha and Achatya (2013) investigated the effect of the bend geometry on the pressure loss and heat transfer. The results showed that the highest pressure drop reduction of 45% was obtained with the bulb with shortest length. Schüler et al. (2011) observed that the use of guide vanes can reduce the pressure drop of about 25% but with almost unchanged heat transfer compared to the case without vanes.

In cooling of gas turbine blades, the blade tip region is one of the most difficult areas to cool because the high temperature gas imposes a large load on the wall. In order to enhance the heat transfer, the outer wall of the U-bend section can be roughened by periodic ribs. Wang et al. (2013) investigated the effects of different pitch ratio of the periodic transversal ribs on the endwall. They found that the presence of ribs increased turbulence levels and altered considerably the flow field. Due to these effects, the highest heat transfer performance was achieved at a pitch ratio of 12. Subsequently, Wang et al. (2014) investigated the effects on heat transfer by various rib configurations at a pitch ratio of 12: transverse ( $90^\circ$ ), angled ( $45^\circ$ ,  $60^\circ$ ) and V-shaped ( $45^\circ$ ,  $60^\circ$ ) with tip pointing both downstream and upstream. They found that the presence of ribs, on the outer wall, enhanced the heat transfer about 2.6 to 3.2 times but the pressure drop penalty also increased by about 6.7 to 7.5. Their results showed that the  $45^\circ$  V-shaped downstream ribs give the best thermal performance.

In this study, an experimental investigation was conducted to investigate the influence of guide vane configurations on the pressure loss and heat transfer in the turn section of a square two-pass channel. Two types of guide vanes are tested. By proper application of guide vanes, the pressure loss over the bend region is substantially reduced while the heat transfer is only moderately changed. To further enhance the heat transfer, the outer wall is roughened by periodic ribs. The combined effect of guide vanes and ribs on the thermal performance is also analyzed. The results can be used to optimize the cooling design for gas turbine blades.

## **Experimental set up and procedure**

The experimental setup of the two-pass channel is presented in **Fig. 1**. The test rig of a U-bend channel consists of three sections: an inlet and outlet section, both of 1.5 m, a turn region of 240 mm. The air flow was supplied by a suction fan connected to the outlet channel while a contracted (area ratio 4:1) bell mouth was installed at the inlet passage to provide a smooth entrance flow. The area of the square duct at both inlet and outlet passes is  $50 \times 50$  mm with a resulting hydraulic diameter  $D_h$  of 50 mm.

Two pressure taps were fixed at the inlet and outlet passages with 340 mm streamwise spacing along the centerline of the channel, as illustrated in Fig. 1. The pressure drop was measured by a stationary micromanometer connected by rubber tubes to the channel. The estimated accuracy is 4%. The pressure drop inside the channel was measured in a condition in which the heater was switched off. The air flow rates in the U-bend section were measured by a rotameter with an accuracy of 3%.

Two different types of guide vanes, named type I and type II, are tested. **Figure 2** shows their detailed dimensions. Guide vanes are made of aluminum with a foil of the thickness of 1 mm and the height of 50 mm, they present the perimeter of  $\frac{1}{4}$  of a circle, with the radius of 17 mm (type I)

and 25 mm (type II) each. The two different vanes are placed in various locations inside the bend zone: in particular, the guide vanes of the type I are at 1/3 or 2/3 of the diagonal on the first or second turn from the inlet, while the guide vanes of the type II are at 1/2 of the same diagonal. Details of the configurations used in the U-bend region are given in **Figure 3**.

Heat transfer on the outer wall of the U bend geometry was also measured. The endwall has the length 240 mm and was covered with a heater and a liquid crystal (LC) film. The LC film was appropriately calibrated (R35C5W, LCR Hallcrest Ltd) in order to measure the local field of temperature on the outer wall. The inner wall length is 140 mm while the gap between the two walls is 50 mm: the effective heat transfer measurement region was 140 mm, or rather the central part of the outer wall. A divider wall with a thickness of 140 mm is used. A CCD camera was placed towards the outer wall, as shown in Fig. 1. The channel wall is made of Plexiglas to provide an optical path to the camera. Throughout the heat transfer measurements, all the parts of the test rig were covered by a black cloth in order to avoid the light noise coming from the surrounding. The coordinate system is chosen in such a manner that the  $x$ -axis is along the streamwise direction,  $y$ -axis is the spanwise direction, and the  $z$ -axis is normal to the outer wall. Plexiglass ribs with a length of 50 mm and a  $3 \times 3$  mm cross section are glued periodically on the endwall. The rib height-to-hydraulic diameter ratio ( $e/D_h$ ) is 0.06 and the pitch-to-rib height ratio ( $P/e$ ) is 12. The rib arrangements investigated are transversal ribs ( $90^\circ$ ) and  $45^\circ$  V tip-downstream pointing ribs.

## Data Reduction

Throughout the experiments, the Reynolds number is defined as:

$$Re = \rho U_0 D_h / \mu \quad (1)$$

where  $U_0$  is the air bulk velocity measured by a rotameter,  $\rho$  and  $\mu$  are, respectively, the density and the dynamic viscosity of the air at the temperature in the laboratory, i.e., 300 K. In this study, the tested Reynolds numbers are 10,000, 18,000 and 26,000.

The pressure drop is normalized by the mainstream fluid dynamic pressure, as presented below:

$$c_p = \Delta P / \rho U_0^2 / 2 \quad (2)$$

where  $\Delta P$  is the pressure drop over the U-bend section. The overall pressure drop is used to calculate the average Darcy friction factor as:

$$f = (\Delta P / L) D_h / \rho U_0^2 / 2 \quad (3)$$

where  $L$  is the streamwise distance between the two pressure taps. The pressure penalty can be normalized by the friction factor for a fully developed turbulent flow in smooth circular tubes, known as the Blasius equation:

$$f_0 = 0.316 / Re^{0.25} \quad (4)$$

The heat transfer coefficient is calculated as:

$$h = (\dot{q}_w - \dot{q}_{loss}) / (T_w - T_0) \quad (5)$$

where  $\dot{q}_w$  is the total electrical heat flux coming from the heater,  $\dot{q}_{loss}$  is the heat conductive and radiative losses (about 8% of the total heat flux),  $T_w$  is the endwall surface temperature obtained by the LC,  $T_0$  is the air bulk temperature at the inlet of the channel, measured by a PT100 thermometer with an accuracy of 0.03 °C.

The Nusselt number is described by:

$$Nu = h D_h / k \quad (6)$$

where  $h$  is the heat transfer coefficient and  $k$  is the air thermal conductivity. The Nusselt number can be normalized by  $Nu_0$ , i.e., the Dittus-Boelter correlation for smooth pipes, Dittus and Boelter (1985):

$$Nu_0 = 0.023 \cdot Re^{0.8} \cdot Pr^{0.4} \quad (7)$$

where  $Pr$  is the Prandtl number.

The thermal performance estimation is based on the same heat transfer surface area and pumping power and is calculated as:

$$\eta = (Nu / Nu_0) / (f / f_0)^{1/3} \quad (8)$$

This parameter estimates the gain in heat transfer against the pressure drop penalty and is well known to identify the best configurations among those presented.

The estimation of uncertainty values has been calculated by the relative analysis method proposed by Moffat (1988), based on a confidence level of 95%. The uncertainty in the pressure drop coefficient was estimated to be 8%, by taking into account several sources of error: the pressure drop measurements of 4%, the bulk velocity and the density of the air of 3% and errors associated with white noise. For the heat transfer coefficients the uncertainty have been estimated to be 10%, considering overall errors which affects the measurements: the loss heat flux, the air bulk temperature and wall temperature, errors associated with the processing of LC images and caused by the lack of repeatability.

## **Results and Discussions**

### **Pressure drop measurements**

**Figure 4** shows the pressure drop measurements in the bend section with 10 different types of guide vane configurations (Fig. 3) and without guide vanes (baseline). Three Reynolds numbers were tested, i.e.,  $Re = 10,000$ ,  $18,000$ , and  $26,000$ . It is clear that the presence of guide vanes can significantly reduce the pressure drop in the bend section compared to the baseline. This can be attributed to the fact that the flow separation near the leading and trailing edges of the inner wall is remarkably attenuated as the flow turns around the bend section. In particular, configuration 9, with 2 guide vanes of II type placed at each diagonal of the bend geometry, shows the best performance, achieving a pressure drop reduction of about 31% at  $Re = 26,000$  compared to the baseline case. In addition, Fig. 4 shows that the configurations 6 and 5, with guide vanes of I and II type at each diagonal of the turn, reach a pressure drop reduction of 30% and 28%, respectively, compared to the baseline at  $Re = 26,000$ . Further inspection of Fig. 4 reveals that the position of guide vanes has a significant impact on the reduction of the pressure drop over the bend section. For example, the configurations 1, 2, and 8, in which the guide vanes are placed at the upstream turning corner, show a pressure drop of almost 20% compared to the baseline at  $Re = 26,000$ , while the configurations 3, 4, and 7, in which the guide vanes are placed at the downstream turning corner, show a pressure

drop of about 6% compared to the baseline at the same Reynolds number. This indicates that the guide vanes are more effective to control the flow separation at the upstream turning corner. On the other hand, the configuration 10, with one guide vane of the type II at 2/3 of each diagonal of the bend region, exhibits a pressure drop reduction of 10% compared to the baseline case. Even though this configuration is less effective in reducing the pressure drop compared to, for instance, configuration 5, it is of interest because the flow is deflected directly to the outer wall by the guide vanes and the heat transfer might be enhanced. This will be considered later.

For the baseline, Fig. 4 shows that the pressure drop coefficient increases monotonously with the increase of Reynolds number. This trend is in line with the results of Rao and Prabhu (2004). The main reason can be attributed to the stronger jet impingement on the outer wall and associated flow separation and recirculation region after the turn in the inner wall. However, with the presence of guide vanes, it is found that all the profiles of the pressure drop coefficient, starting at  $Re = 10,000$ , first fall down at  $Re = 18,000$  and then rise up at  $Re = 26,000$ , indicating that the flow structures are affected by the Reynolds numbers. The reason is not clear yet, but more studies, especially the PIV measurements, will be performed to investigate the flow physics in the bend section with various guide vane configurations.

In the following, the heat transfer characteristics on the outer wall with and without guide vanes will be examined. Only the configurations 5, 6, 9, and 10 and the baseline are tested.

### **Heat transfer with guide vanes**

**Figure 5** displays the profiles of the spanwise-averaged Nusselt number on the outer wall along the streamwise direction at  $Re = 26,000$ . Compared to the baseline, it is found that all the guide vane configurations reduce the heat transfer on the endwall. This can be explained by the fact that the flow is deflected away from the outer wall and the jet impingement effect is thus attenuated. However, the present study is not consistent with the results of Schüler et al. (2011), in which they

found that heat transfer is almost unchanged in the turn region when the guide vanes were introduced. In addition, the  $\overline{Nu}$  profiles bear some similarity for all the tested guide vane configurations. With the presence of guide vanes, all the profiles show a local minimum at  $x/D_h = 1.5$ . However, for the baseline case, the position of the local minimum is shifted upstream at  $x/D_h = 1.2$ , indicating that the boundary layer on the outer wall is significantly modified as the guide vanes are fitted into the bend section. Compared to the baseline, the configuration 6 provides the lowest heat transfer and the configuration 10 produces almost an unchanged heat transfer.

**Figure 6** presents the area-averaged Nusselt number ratio versus friction factor ratio for the baseline case and the selected configurations of guide vanes, i.e., 5, 6, 9, and 10 inside the bend at  $Re = 26,000$ . The study shows that all the tested configurations reduce the pressure drop penalty and also the heat transfer on the endwall compared to the baseline case. For the baseline case, the heat transfer is enhanced by a factor of about 1.95 to 2, while the pressure drop penalty increases about 38 times compared to a smooth tube, which is in agreement with Wang et al. (2014). In particular, configuration 9 shows the best performance in terms of the pressure drop, with a friction factor ratio of about 26, but with a low Nusselt number ratio  $Nu/Nu_0 = 1.85$  (i.e., less than 7% with respect to the baseline). Configurations 5 and 6 are effective in reducing the pressure drop but at a high heat transfer cost. Note that configuration 10 has a similar heat transfer capacity to that of the baseline case but with a relatively noticeable pressure drop reduction (about 10%).

### **Heat transfer with combined guide vanes and ribs**

Ribs are devices used in heat exchangers to promote heat transfer. By strongly disturbing the boundary layer, the heat transfer can be significantly enhanced. In order to investigate the combined effect of guide vanes and ribs on the outer wall heat transfer, configurations 5 and 10 are selected as typical guide vane arrangements, and transverse ( $90^\circ$ ) ribs and V  $45^\circ$  downstream pointing ribs are used in this study. The rib height is 3 mm and the pitch-to-height ratio is 12.

**Figure 7** displays the heat transfer distributions on the outer wall with configuration 5 of the guide vanes inside the bend region and transverse rib arrangement at  $Re = 26,000$ . The black strips represent the position of the ribs. Compared with the baseline case, see Wang et al. (2013), the presence of ribs enhances the heat transfer significantly. The maximum heat transfer area is reached at  $0.4 < x/D_h < 0.8$ . Further downstream, the heat transfer undergoes a gradual decrease due to the increased boundary layer thickness. **Figure 8** shows the heat transfer distributions on the outer wall with configuration 10 of the guide vanes and transverse rib arrangement. Even though the maximum heat transfer is also observed in the region  $0.4 < x/D_h < 0.8$ , the heat transfer in the downstream region decays much quicker than that in Fig. 7 and is similar to the case where only the ribs were present in the bend section, see Wang et al. (2013).

**Figure 9** displays the heat transfer distributions on the outer wall for configuration 5 of the guide vanes inside the bend region and V-45° downstream pointing rib arrangement, at  $Re = 26,000$ . The high heat transfer areas in this case are located at the zones near the top ( $y/D_h > 0.3$ ) and bottom ( $y/D_h < -0.3$ ) walls, where the secondary flow induced by the ribs is directed towards the outer wall. In the middle region ( $-0.2 < y/D_h < 0.2$ ) a low heat transfer value is observed, due to the fact that secondary flows leave from the bottom wall. It is interesting to note, according to Wang et al. [20], that the V - 45° downstream pointing rib arrangement generates two counterrotating vortices with the same direction of the Dean vortices due to the bend geometry. **Figure 10** displays the heat transfer distributions on the outer wall for configuration 10 of the guide vanes inside the bend region and V-45° downstream pointing rib arrangement. Basically the heat transfer patterns are similar to those of Fig. 9. However, the secondary flows induced by the position of the guide vanes are stronger than that of the previous case. For this reason, Fig. 10 presents a bigger high heat transfer area close the top ( $y/D_h > 0.2$ ) and bottom ( $y/D_h < -0.2$ ) outer wall.

**Figure 11** presents the area-averaged Nusselt number ratio versus friction factor ratio for ribbed walls with guide vanes inside the bend section. The combined use of ribs and guide vanes improve the heat transfer ( $2.2 < Nu/Nu_0 < 2.7$ ) compared to the baseline ( $Nu/Nu_0 = 1.95$ ). For all the configurations studied, the V - 45° downstream pointing ribs coupled with configuration 5 of the guide vanes provides the best trade-off, achieving a high Nusselt number ratio ( $Nu/Nu_0 = 2.6$ ) with a small gain in pressure drop ( $f/f_0 = 36$ ), while the transverse ribs coupled with the configuration 10 of the guide vanes produces the largest pressure drop ( $f/f_0 = 48$ ) but with a moderate increase of heat transfer ( $Nu/Nu_0 = 2.2$ ) compared to the baseline.

**Figure 12** shows the thermal performance for ribbed walls with guide vanes inside the bend section at  $Re = 26,000$ . Obviously, all the tested cases have a higher thermal performance than the baseline ( $\eta = 0.58$ ). In particular, the V - 45° downstream pointing ribs coupled with configuration 5 of the guide vanes exhibit the best thermal performance ( $0.75 < \eta < 0.8$ ). The 90° ribs with configuration 5 of the guide vanes has higher thermal performance ( $\eta = 0.72$ ) than 90° ribs with configuration 10 of the guide vanes ( $\eta = 0.62$ ). This is probably due to the position of the guide vanes inside the turn.

## Conclusions

Heat transfer and pressure drop have been experimentally determined in the U-bend section of a two-pass channel with and without the presence of guide vanes and ribs:

- The use of guide vanes can effectively reduce the pressure drop but with the cost of lower heat transfer compared to the baseline. Comparison of 10 different configurations of guide vanes was presented and the configuration 9 reduced the pressure penalty up to 31%. In particular, the guide vane is more effective in reducing the pressure loss when placed in the upstream turning corner than in the downstream turning corner.

- With a particular type of guide vanes (i.e., configurations 5 and 10) and the presence of ribs on the endwall (i.e., 90° ribs and V - 45° downstream pointing ribs), the heat transfer is enhanced to a maximum of 35% for V - 45° downstream, coupled with configuration 10 of the guide vanes, but at the penalty of a higher pressure drop compared to the baseline case.
- The combination of ribs and guide vanes allows the thermal performance to be significantly increased. Thermal performance evaluation shows that the V - 45° downstream pointing endwall ribs coupled with configuration 5 of the guide vanes gave the best thermal performance.

## Acknowledgments

This research work has been financially supported by the Swedish Research Council (VR) and the Swedish Energy Agency. Susanna Cimina was a visiting PhD student at Lund University and the measurements were conducted during that time period.

## References

- Chen, W., Ren, J., and Jiang, H., (2011) Effect of Turning Vane Configurations on Heat Transfer and Pressure Drop in a Ribbed Internal Cooling System, *ASME J. Turbomachinery*, vol. **133**(4), 041012.
- Coletti, F., Verstraete, T., Bulle, J., Van der Wielen, T., Van den Berge, N., and Arts, T., (2013) Optimization of a U-Bend for Minimal Pressure Loss in Internal Cooling Channels—Part II: Experimental Validation, *ASME J. Turbomachinery*, vol. **135**(5), 051016.
- Dittus, F. W., and Boelter, L. M. K., (1985) Heat Transfer in Automobile Radiators of the Tubular Type, *Int. Communications in Heat and Mass Transfer*, vol. **12**(1), pp. 3-22.
- Ekkad, S. V., and Han, J. C., (1997) Detailed Heat Transfer Distributions in Two-Pass Square Channels with Rib Turbulators, *Int. J. Heat and Mass Transfer*, vol. **40**(11), pp. 2525-2537.

Fan, C. S., and Metzger, D. E., (1987) Effects of Channel Aspect Ratio on Heat Transfer in Rectangular Passage Sharp 180-deg Turns, *32nd International Gas Turbine Conference and Exhibition, paper no 87-GT-13*.

Han, J. C., (2004) Recent Studies in Turbine Blade Cooling, *Int. J. Rotating Machinery*, vol. **10**(6), pp. 443-457.

Han, J. C., Dutta, S., and Ekkad, S., (2012) *Gas Turbine Heat Transfer and Cooling Technology*, CRC Press.

Luo, J., and Razinsky, E. H., (2009) Analysis of Turbulent Flow in 180 deg Turning Ducts with and without Guide Vanes, *ASME J. Turbomachinery*, vol. **131**(2), 021011.

Metzger, D., Fan, C., and Plevich, C., (1988) Effects of Transverse Rib Roughness on Heat Transfer and Pressure Losses in Rectangular Ducts with Sharp 180 degree Turns, *26<sup>th</sup> Aerospace Sciences Meeting, paper no AIAA-88-0166, Reno, NV*.

Metzger, D. E., Plevich, C. W., and Fan, C. S., (1984) Pressure Loss through Sharp 180 deg Turns in Smooth Rectangular Channels, *J. Engineering for Gas Turbines and Power*, vol. **106**(3), 677-681.

Metzger, D. E., & Sahm, M. K., (1986), Heat Transfer around Sharp 180-deg Turns in Smooth Rectangular Channels. *ASME J. Heat Transfer*, vol. **108**(3), pp. 500-506.

Moffat, R. J., (1988) Describing the Uncertainty in Experimental Results, *Exp. Thermal Fluid Sci.*, **1**, pp. 3–17.

Rao, D. V., Babu, C. S., and Prabhu, S. V., (2004) Effect of Turn Region Treatments on the Pressure Loss Distribution in a Smooth Square Channel with Sharp 180 Bend, *Int. J. Rotating Machinery*, vol. **10**(6), pp. 459-468.

Rao D, V. R., and Prabhu, S. V., (2004) Pressure Drop Distribution in Smooth and Rib Roughened Square Channel with Sharp 180 Bend in the Presence of Guide Vanes, *Int. J. Rotating Machinery*, vol. **10**(2), pp. 99-114.

Saha, K., and Acharya, S., (2013) Effect of Bend Geometry on Heat Transfer and Pressure Drop in a Two-Pass Coolant Square Channel for a Turbine, *ASME J. Turbomachinery*, vol. **135**(2), 021035.

Schabacker, J., Boelcs, A., and Johnson, B. V., (1998) PIV Investigation of the Flow Characteristics in an Internal Coolant Passage with Two Ducts connected by a Sharp 180 deg Bend, In *Proceedings of the ASME Turbo Expo 1998 Conference*, paper no 98-GT-544.

Schüler, M., Zehnder, F., Weigand, B., von Wolfersdorf, J., and Neumann, S. O., (2011) The Effect of Turning Vanes on Pressure Loss and Heat Transfer of a Ribbed Rectangular Two-Pass Internal Cooling Channel, *ASME J. Turbomachinery*, vol. **133**(2), 021017.

Son, S. Y., Kihm, K. D., and Han, J. C., (2002) PIV Flow Measurements for Heat Transfer Characterization in Two-Pass Square Channels with Smooth and 90 Ribbed Walls, *Int. J. Heat Mass Transfer*, vol. **45**(24), pp. 4809-4822.

Sunden, B., and Xie, G., (2011) Gas Turbine Blade Tip Heat Transfer and Cooling: A Literature Survey, *Heat Transfer Engineering*, vol. **31**(7), pp. 527-554.

Wang, C., Wang, L., Sunden, B., (2014) An Experimental Study of Heat Transfer in a Turn Region of a U-bend Channel with Various Ribs, *Proceedings of the 15th International Heat Transfer Conference*, paper no IHTC15-8864, Kyoto, Japan.

Wang, L., Ghorbani-Tari, Z., Wang, C., Wu, Z., and Sundén, B., (2013) Endwall Heat Transfer at the Turn Section in a Two-Pass Square Channel with and without Ribs, *J. Enhanced Heat Transfer*, vol. **20**(4).

## Figure Captions

**Fig. 1** A 3D (*a*) and 2D (*b*) view of the experimental setup: bend geometry

**Fig. 2** Specification of the guide vanes: (*a*) type I,  $R = 25$  mm, (*b*) II type,  $R=17$  mm.

**Fig. 3** Tested configurations.

**Fig. 4** Pressure drop coefficient versus Reynolds number for baseline case and configurations with guide vanes.

**Fig. 5** Streamwise distributions of Nu for selected configurations of guide vanes at  $Re = 26,000$ .

**Fig. 6** Area-averaged Nusselt number ratio versus friction factor ratio for selected configurations of guide vanes at  $Re= 26,000$ .

**Fig. 7** Local Nusselt number distribution on the endwall with  $90^\circ$  ribs and configuration 5 of guide vanes,  $Re=26,000$

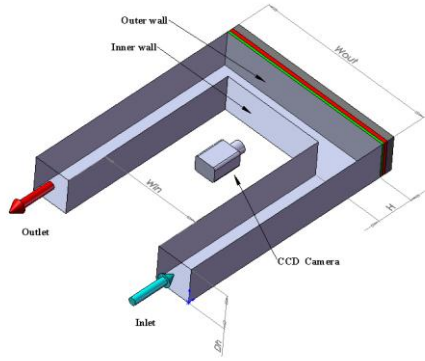
**Fig. 8** Local Nusselt number distribution on the endwall with  $90^\circ$  ribs and configuration 10 of guide vanes,  $Re=26,000$

**Fig. 9** Local Nusselt number distribution on the endwall with  $45^\circ$  V shaped downstream ribs and configuration 5 of guide vanes,  $Re=26,000$

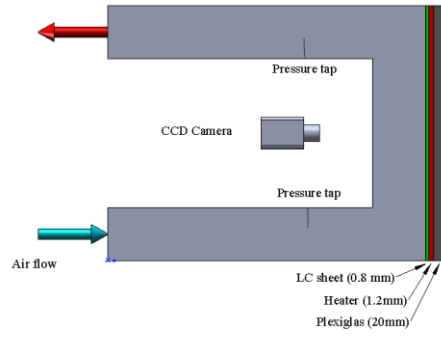
**Fig. 10** Local Nusselt number distribution on the endwall with  $45^\circ$  V shaped downstream ribs and configuration 10 of guide vanes,  $Re=26,000$

**Fig. 11** Area-averaged Nusselt number ratio versus friction factor ratio for the combination of guide vanes and ribs at  $Re = 26,000$ .

**Fig. 12** Thermal performance comparison for the combination of guide vanes and ribs.

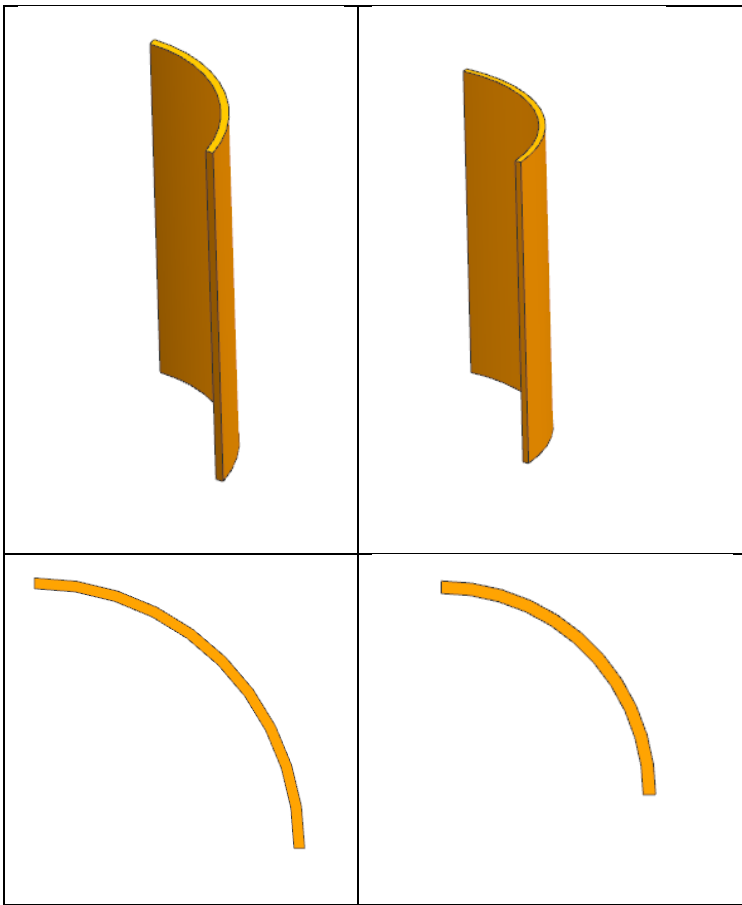


(a)



(b)

**Fig. 1** A 3D (a) and 2D (b) view of the experimental setup: bend geometry



(a)

(b)

**Fig. 2** Specification of the guide vanes: (a) type I,  $R = 25$  mm, (b) II type,  $R = 17$  mm.

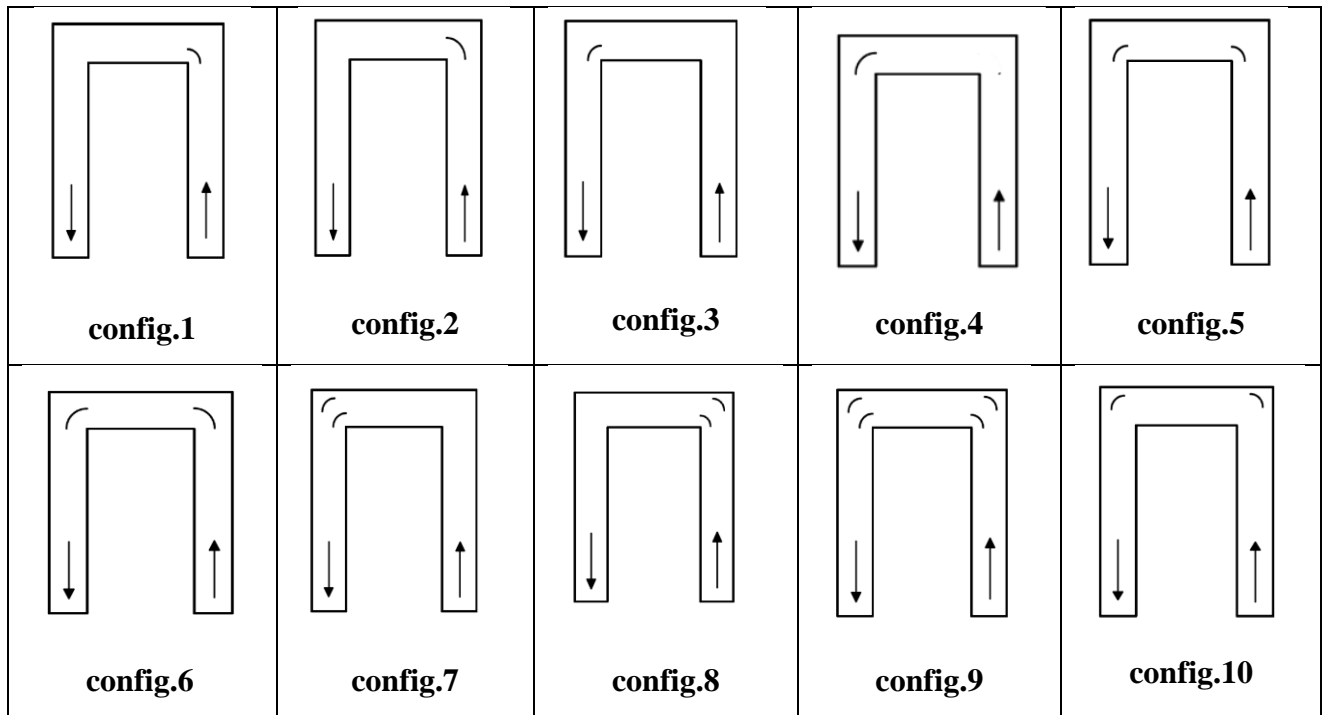


**Fig. 3** Tested configurations.

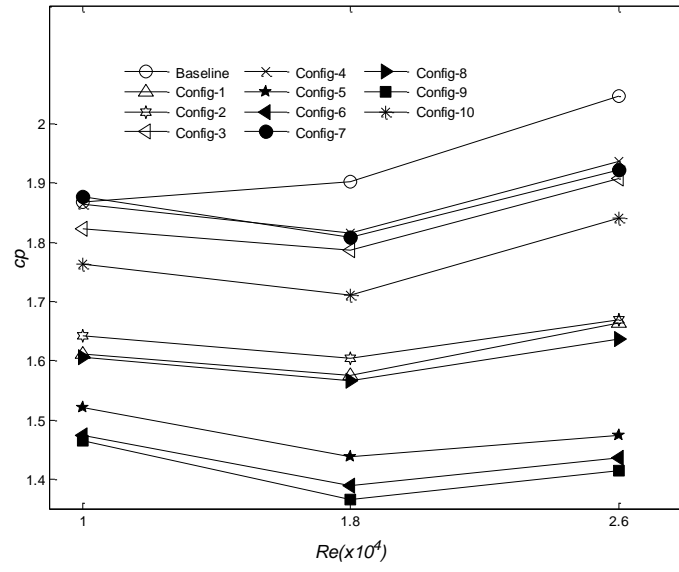


**Fig. 4** Pressure drop coefficient versus Reynolds number for baseline case and configurations with guide vanes.

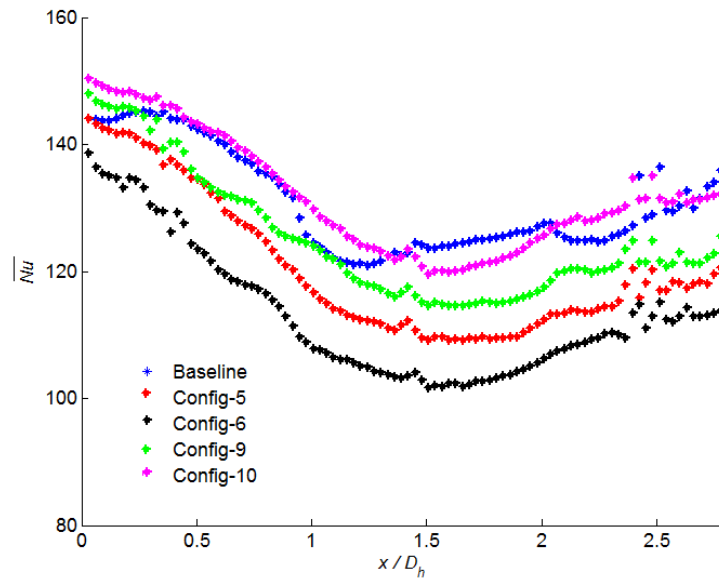


**Fig. 5** Streamwise distributions of Nu for selected configurations of guide vanes at  $Re = 26,000$ .

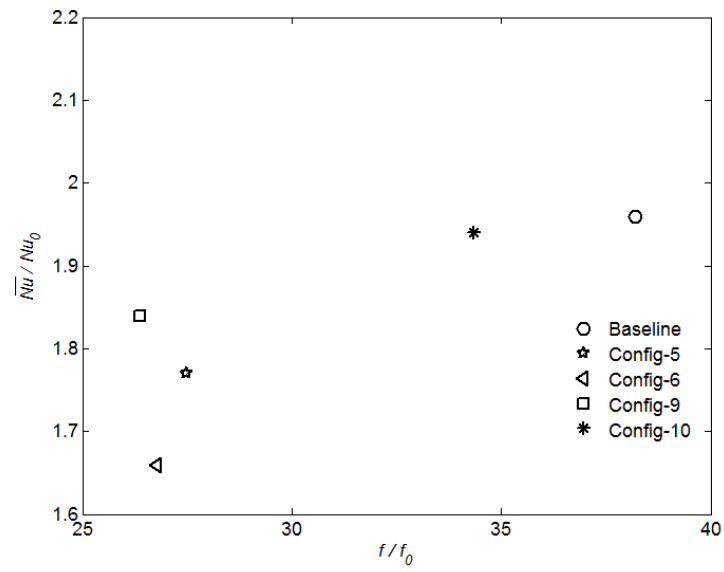


**Fig. 6** Area-averaged Nusselt number ratio versus friction factor ratio for selected configurations of guide vanes at  $Re= 26,000$ .

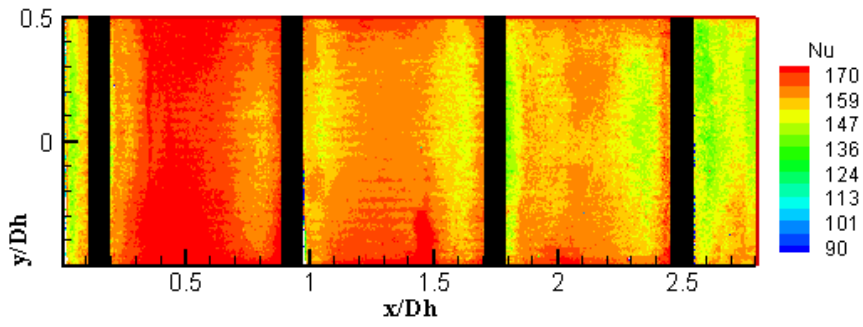


**Fig. 7** Local Nusselt number distribution on the endwall with  $90^\circ$  ribs and configuration 5 of guide vanes at  $Re=26,000$ .

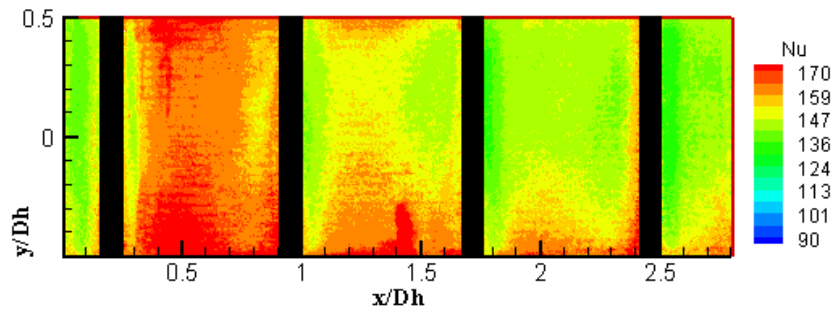


**Fig. 8** Local Nusselt number distribution on the endwall with 90° ribs and configuration 10 of guide vanes at  $Re=26,000$ .

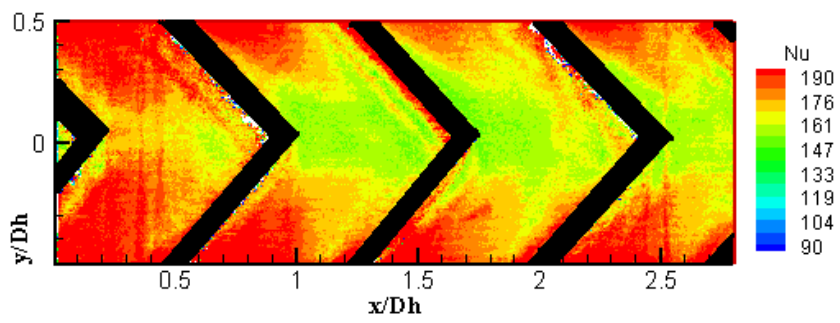


**Fig. 9** Local Nusselt number distribution on the endwall with  $45^\circ$  V shaped downstream ribs and configuration 5 of guide vanes at  $Re=26,000$ .

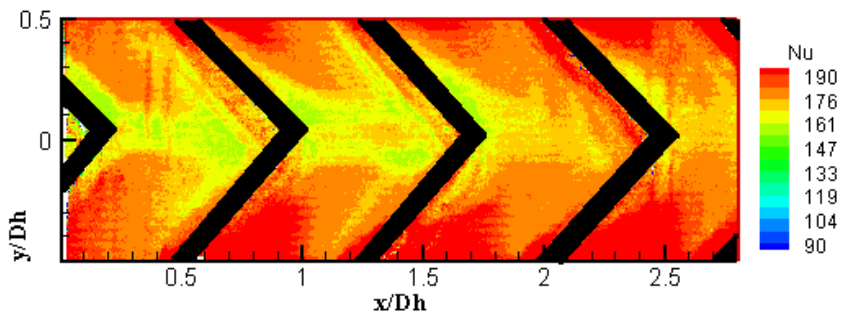


**Fig. 10** Local Nusselt number distribution on the endwall with  $45^\circ$  V shaped downstream ribs and configuration 10 of guide vanes,  $Re=26,000$

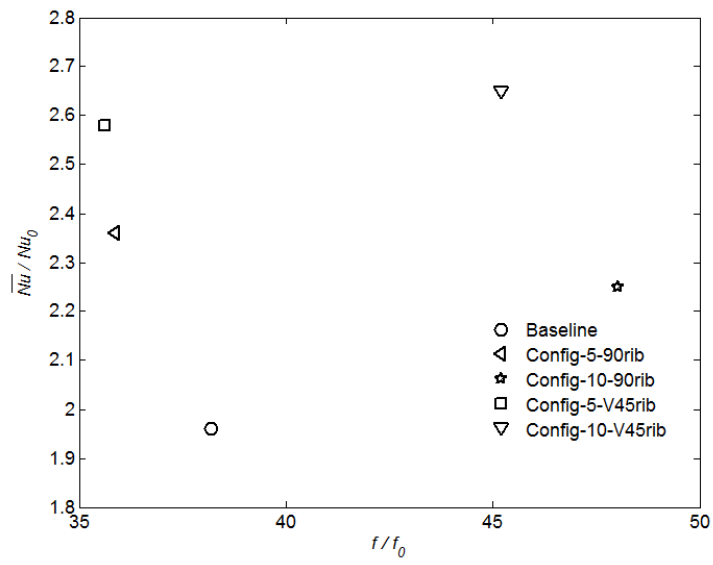


**Fig. 11** Area-averaged Nusselt number ratio versus friction factor ratio for the combination of guide vanes and ribs at  $Re = 26,000$ .

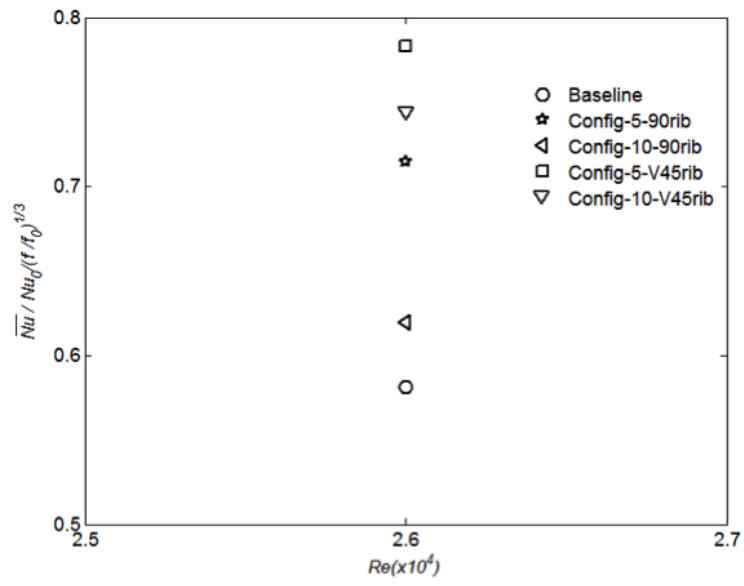


**Fig. 12** Thermal performance comparison for the combination of guide vanes and ribs.